www.czasopisma.pan.pl PAN POLSKA AKADEMIA NAUK www.journals.pan.pl

A R C H I V E S O F M E T A L L U R G Y A N D M A T E R I A L S

Volume 59 2014 Issue 2

DOI: 10.2478/amm-2014-0102

J. MAŁECKA*

OXIDATION RESISTANCE OF AlCrN COATING DEPOSITED ON Ti-46Al-7Nb-0.7Cr-0.1Si-0.2Ni ALLOY

ODPORNOŚĆ NA UTLENIANIE POWŁOKI AlCrN NANIESIONEJ NA STOP Ti-46Al-7Nb-0,7Cr-0,1Si-0,2Ni

This article presents the results of research on resistance to isothermal oxidation of Ti-46Al-7Nb-0,7Cr-0,1Si-0,2Ni alloy with AlCrN layer applied. The reference material was a Ti-46Al-7Nb-0,7Cr-0,1Si-0,2Ni alloy in initial state without any coating deposited. The protective coating was deposited by PVD process. Attempts at isothermal oxidation in air were performed at 900 and 950°C during 250h. Measurements of the samples' mass were taken with the accuracy of 10^{-4} g. An analysis of the obtained results was made: chemical composition analysis, phase analysis of the deposited coating and chemical composition analysis of the alloy surface with the coating deposited after oxidation tests. In the case of the oxidation of alloy in initial state, pronouncedly higher mass gain and "deferred" scale chipping was noticed. The deposited AlCrN coating significantly reduces spalling processes and makes for lesser mass gain of the oxidized alloy.

Keywords: intermetallics, high temperature corrosion, oxidation

W artykule przedstawiono wyniki badań odporności na utlenianie izotermiczne stopu Ti-46Al-7Nb-0,7Cr-0,1Si-0,2Ni z naniesioną powłoką AlCrN. Materiałem referencyjnym był stop Ti-46Al-7Nb-0,7Cr-0,1Si-0,2Ni w stanie wyjściowym, bez naniesionej powłoki. Powłoka ochronna naniesiona została w procesie PVD. Próby izotermicznego utleniania w powietrzu przeprowadzono w temperaturze 900 i 950°C w czasie 250h. Pomiary masy próbek przeprowadzane były z dokładnością 10^{-4} g. Dokonano analizy uzyskanych wyników: składu chemicznego i fazowego naniesionej powłoki oraz składu chemicznego powierzchni stopu z naniesioną powłoką po testach utleniania. Stwierdzono, w przypadku utleniania stopu w stanie wyjściowym, wyraźnie większe przyrosty masy i „zwłoczne" odpryskiwanie zgorzeliny. Naniesiona powłoka AlCrN zdecydowanie ograniczyła procesy odpryskiwania zgorzeliny oraz przyczyniła się do mniejszego przyrostu masy utlenianego stopu.

1. Introduction

Alloys with ordered intermetallic phases have found broad application as structural materials meant for operation in elevated temperature and aggressive chemical environment. Alloys with the structure composed of intermetallic phases with Ti-Al arrangement are a very attractive material due to their properties, which enable their implementation in many areas of application: in space, aviation or automotive industry [1]. High strength, low density, good creep resistance are the main assets of Ti-Al intermetallic alloys [2]. Ti aluminides are particularly popular as materials used in the production of gas turbine components and they promise to improve reliability, lower the emission, lengthen the life and lower the cost of manufacturing [3]. The efficient application of these alloys is however restricted by their low plasticity at the room temperature and insufficient resistance to oxidation above 700°C. During the high temperature oxidation, a protective coating of Al_2O_3 is not formed whereas the coating consisting of the mixture of Al_2O_3 and TiO_2 does not possess sufficient protective properties [4÷5]. Current research studies principally concern the improvement of the oxidation resistance of these alloys. This issue is presently the main problem, limiting the application of the examined alloys. The improvement in the oxidation resistance is possible through modifying the chemical composition with suitable alloying additives [6÷13], which, however, adversely affect the plasticity. Therefore, the best way to improve Ti-Al alloy oxidation resistance is the application of appropriate protective coatings. The current literature widely presents achievements concerning the protective coatings that improve high temperature resistance of Ti-Al intermetallic alloys [14÷19]. The research work shown in this paper investigated an AlCrN coating obtained in PVD process.

2. Material and methods

The tests were performed on a multi-component alloy Ti-46Al-7Nb-0,7Cr-0,1Si-0,2Ni with the content of 46%at Al, 7%at Nb, 0,7%at Cr, 0,1%at Si and 0,2%at Ni purchased from Flowserve Corporation Titanium and Reactive Metals Foundry (USA). The samples of alloy with dimensions of ≈20×15×2 mm were polished with 800 grade abrasive paper and subsequently degreased in acetone. Surface parameters of the samples after polishing were determined by means of

* OPOLE UNIVERSITY OF TECHNOLOGY, FACULTY OF MECHANICAL ENGINEERING, 5 MIKOŁAJCZYKA STR., 45-271 OPOLE, POLAND

Hommel Tester 1000 profilometer with LV15 measuring head. The roughness of the surface prepared in this manner was Ra =0,06μm. A layer of AlCrN coating was deposited on such a surface using Physical Vapor Deposition – PVD. The solid state coating material of high purity underwent vaporising as a result of heat or ion sputtering. Simultaneously, reactive gas was introduced and a compound was formed with the metal vapour which deposited on the surface in form of thin, highly adhesive layer. In order to obtain equal thickness of the coating, the substrates were rotating at a steady speed around a few axes. The samples with coating obtained in this manner underwent tests of isothermal oxidation at the temperature of 900°C and 950°C during 250 hours in hot air atmosphere. The station for oxidation consisted of a furnace linked to a computer registering the oxidation temperature. Mass changes due to oxidation processes was controlled by a precision scale with the accuracy of 10^{-4}g . The humidity of air was measured by H883T hygrometer and amounted to 39% whereas the temperature of the recording was 15°C. The temperature of air during oxidation fluctuated in the range of 18,2÷21,1°C. For comparison, the reference alloy were samples of the alloy without the coating. The study performed included the analysis of chemical and phase composition of the coating directly after PVD process. Additionally microstructural research was carried out. For this purpose scanning electron microscopy (SEM) methods were used (with secondary electron (SE) emissions and back-scattered electron (BSE) emissions); X-ray phase analysis XRD (X-ray diffraction) and chemical composition analysis by means of EDX (energy-dispersive X-ray spectroscopy).

3. Results and discussion

The structure of the Ti-46Al-7Nb-0,7Cr-0,1Si-0,2Ni alloy can be specified as duplex [13]. Microphotography image of the AlCrN coating after PVD process presented on the cross-section of the sample was shown in Fig. 1. The produced coating was characterized by a single-layer structure. The chemical composition of the marked spots was shown in Fig. 2.

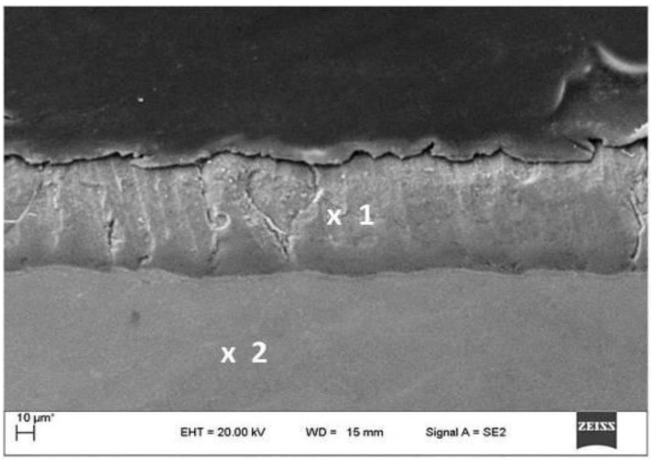

Fig. 1. Cross-section of the sample coated with AlCrN

The analysis of the phase composition was presented in Fig. 3. It is obvious that the basic phase elements are AlCrN, which is confirmed by the picture of the deposited coating. Beside the fundamental elements, metallic substrate peaks are visible i.e. intermetallic γ-TiAl and α_2-Ti_3Al phase. It is easily explicable as the formed coating is thin enough for the metallic substrate to produce its lines. The thickness of the coating was circa 60 μm.

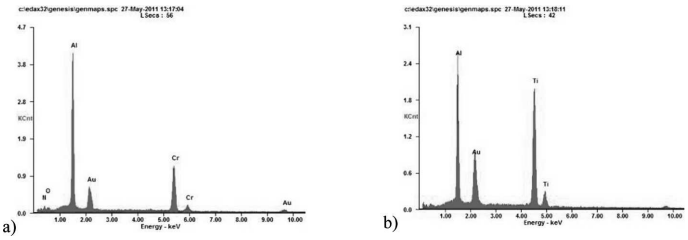

Fig. 2. EDX analysis results: (a) in place 1 according to Fig. 1 and (b) in place 2 according to Fig. 1

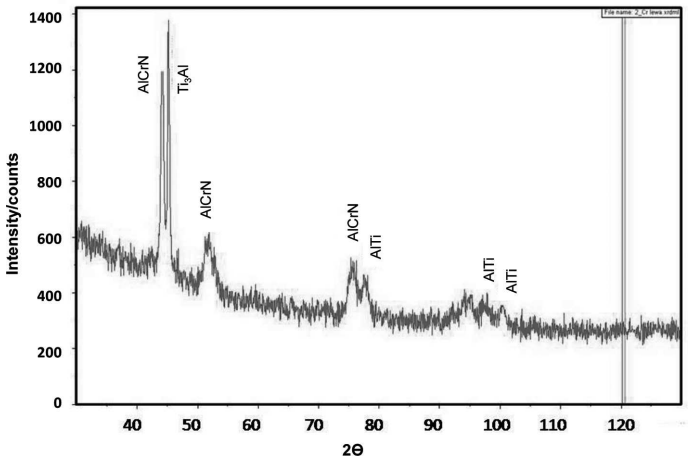

Fig. 3. XRD microanalysis result of Ti-46Al-7Nb-0.7Cr-0.1Si-0.2Ni alloy coated with AlCrN

The distribution of elements on the section of the alloy coated with AlCrN is shown in Fig. 4. The areas rich in Ti and Al are visible on the alloy substrate and Al and Cr in the place where the coating was deposited.

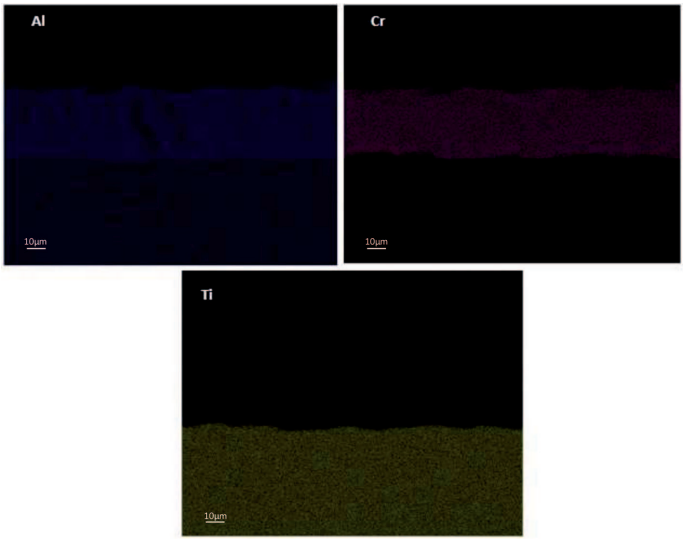

Fig. 4. The distribution of elements on the section of the Ti-46Al-7Nb-0,7Cr-0,1Si-0,2Ni alloy coated with AlCrN

In oxidation trials, the material destruction process includes the formation of oxides in heating cycles, chipping during cooling and holding in the room temperature. The course of oxidation of the oxidized alloy was presented in Fig. 5.

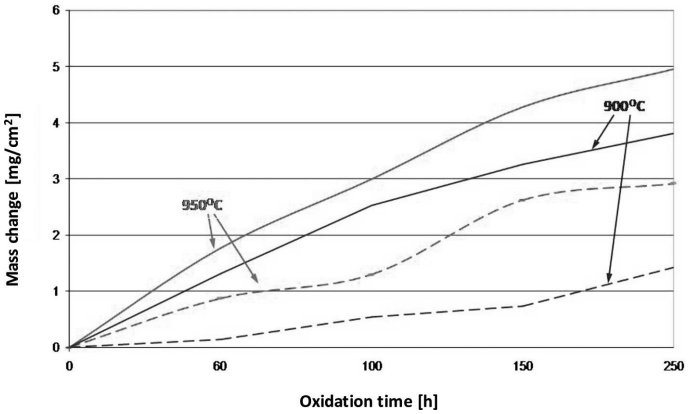

Fig. 5. The mass change of Ti-46Al-7Nb-0,7Cr-0,1Si-0,2Ni oxidized isothermally at 900°C and 950°C (continuous curves for initial state alloy and dashed curves for the alloy coated with AlCrN)

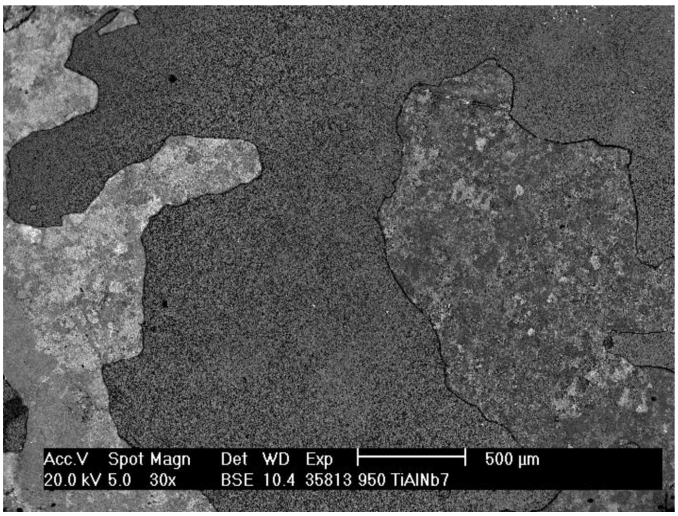

Fig. 6. Chip damage on the uncoated alloy surface

AlCrN coatings exhibited significantly reduced mass gain compared to the bare substrate material. Isothermal oxidation at 900°C and 950°C during 250 hours causes mass gain, which intensifies at 950°C both in the case of alloy in initial state as well as for samples with the coating of AlCrN. However, during oxidation tests, considerable decrease in mass gain was observed for the alloy coated with AlCrN. The mass gain of the coated alloy sample after 250 hours of heating at 900°C is about 1.3 mg/cm^2 and about 2.9 mg/cm^2 at 950°C. The scale forming on the surface of samples was tightly attached to the substrate and did not chip either immediately after the test not later. Whereas the mass gain for the uncoated alloy is respectively 3.81 mg/cm^2 and 4.95 mg/cm^2. The uncoated samples observed immediately after the completion of isothermal oxidation were characterized by a good adhesion of products with the metallic substrate up to 100 hours of oxidation. After 250 hours, chipping of scale fragments was observed while cooling down to the room temperature. For the higher temperature (950°C), chipping was observed even after shorter times. Along with the lengthening of the oxidation time, the chipping of the oxide layer intensifies and it becomes severe (Fig. 6). Despite the fact that immediately after finishing the tests the products stuck to the surface of the samples, just during 24 hours such amount of products subsequently chipped that only tiny micro-islets remained on the metallic substrate of the samples, leaving them almost completely unprotected after the oxidation in air.

The oxidation of the Ti-46Al-7Nb-0,7Cr-0,1Si-0,2Ni alloy results not only in scale formation, but also alterations in the substrate caused by ex-core diffusion of alloying elements and by forming phases and solid solutions due to in-core diffusion of oxygen and nitrogen.

Previous research dealt with determining the area of resistance to high temperature oxidation of Ti-46Al-7Nb-0,7Cr-0,1Si-0,2Ni alloy without protective coatings [12÷13]. Based on the investigations and analyses of fractures and cross-sections of the oxidized alloy, it can be concluded that the produced layer is characterized by an identical sequence of sublayers regardless of the oxidation temperature. Nevertheless, a rise in the temperature of the process makes the oxide scale grow thicker. The following sequence of sublayers may be distinguished (Fig. 7):

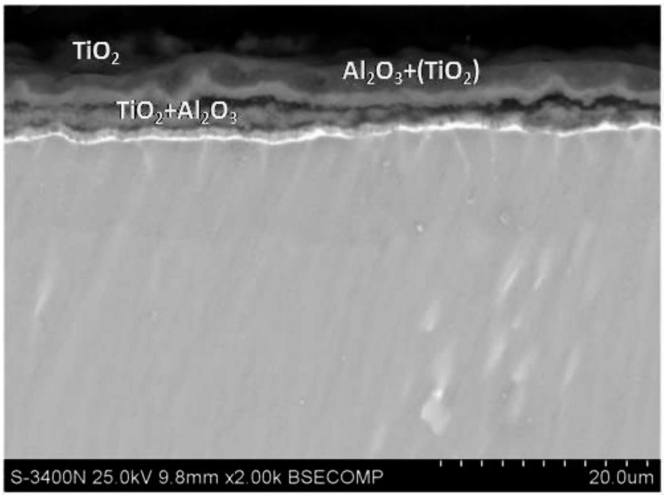

Fig. 7. Cross-section of products and metallic sublayer of the oxidized Ti-46Al-7Nb-0,7Cr-0,1Si-0,2Ni alloy

1. Outer layer made of columnar crystallites of rutile TiO_2. Columnar crystallites growing in various directions can be observed on the oxidized surface. On a free surface these crystallites grow not only as a result of ex-core diffusion of titanium ions, but also due to surface diffusion. This fact causes that they are situated perpendicular and at different angles to the surface they grow out of.

2. Immediately under columnar crystallites of rutile exists another sublayer, which returns a grey-black heterogeneous contrast in BSE scan images. It is a two-phase mixed layer rich in Al_2O_3 also containing TiO_2 oxides.

3. Yet another, the third sublayer extends as far as the metallic substrate boundary. It is a multi-phase layer composed of Al_2O_3, TiO_2 and oxides of metal originating from the composition of the alloy.

4. In the area of the metallic substrate of the examined alloy diffusive processes occur as well, and therefore a dis-

continued micro-band, rich in the alloying elements with high atomic numbers, forms in the metallic substrate brightly contrasting in BSE.

The observation alone of the surface of alloy samples isothermally oxidized in air is enough to determine that oxidation products are different for the coated and uncoated alloy. During the oxidation of the initial state Ti-46Al-7Nb-0,7Cr-0,1Si-0,2Ni alloy, columnar crystallites growing in various directions can be observed on the oxidized surface (Fig. 8). The analysis of the structure and composition of the isothermal air oxidation products allows concluding that the product covering the surface contains more titanium compared to the aluminium content (Fig. 9), which indicates that the product formed on the outer surface is rutile crystallites TiO_2, generated as a result of ex-core diffusion of titanium.

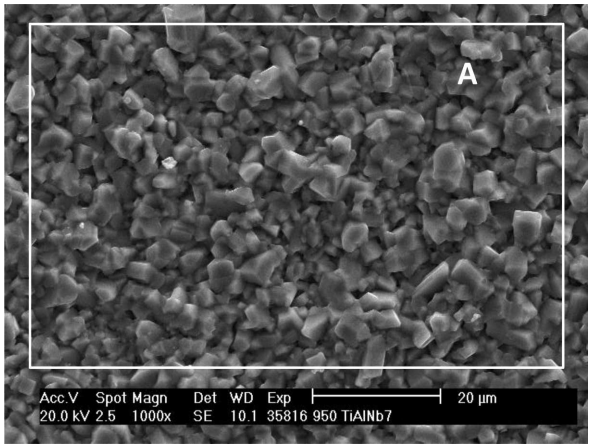

Fig. 8. The surface Ti-46Al-7Nb-0,7Cr-0,1Si-0,2Ni after 60 hours of isothermal oxidation in air at 900°C

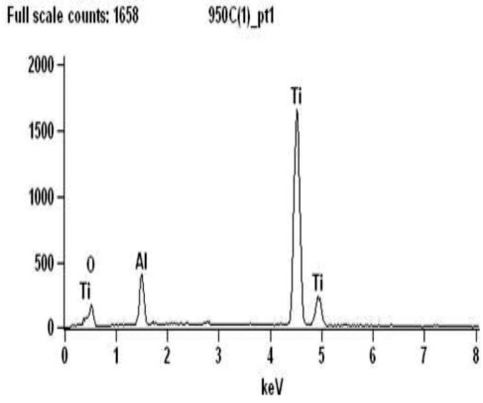

Fig. 9. EDX analysis results of the area inside the rectangle # A according to Fig. 8

The layer of products formed on the Ti-46Al-7Nb-0,7Cr-0,1Si-0,2Ni alloy coated with AlCrN has a completely different structure. The structure of the scale surface formed upon the oxidation of the alloy coated with AlCrN (Fig. 10) has a totally different appearance than that of the alloy in the as-as state. It was noticed that the alloy's surface after the oxidation is mostly a coherent, non-chipping layer containing Al and Cr (Fig. 11). Rutile efflorescences appear locally (Fig. 12÷13). As it can be seen, they do not form on the entire surface of the alloy, growing only locally. The micro-zones reveal differences in composition. It is reflected in the surface sectors in Fig. 10 where the selected A zone is clearly enriched with aluminium and chromium (Fig. 14a), which points to the presence of deposited AlCrN coating, whereas in the composition of B zone, apart from aluminium and chromium, titanium is mostly present (Fig. 14b). This analysis may explain the appearance of rutile efflorescences. The deposited coating of AlCrN on Ti-46Al-7Nb-0,7Cr-0,1Si-0,2Ni alloy decreases the range of covering the alloy's surface with TiO_2 rutile, contributing to decreasing the rate of oxidation of the examined alloy.

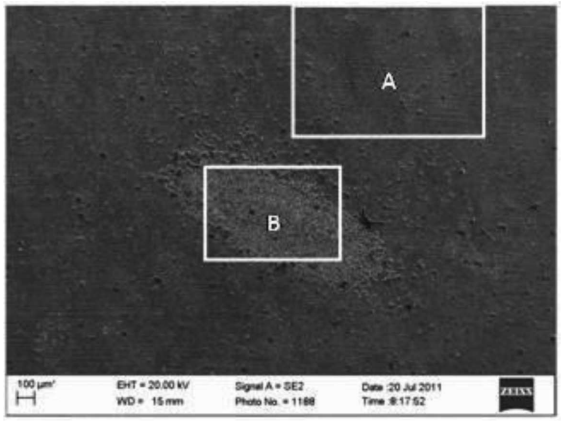

Fig. 10. The surface Ti-46Al-7Nb-0,7Cr-0,1Si-0,2Ni with AlCrN layer applied after isothermal oxidation in air at 950°C

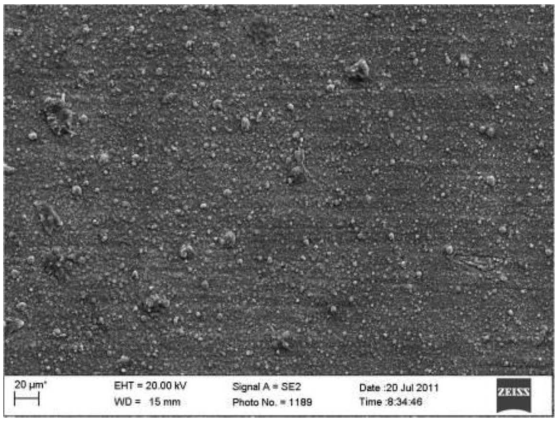

Fig. 11. The surface inside the rectangle #A according to Fig. 10

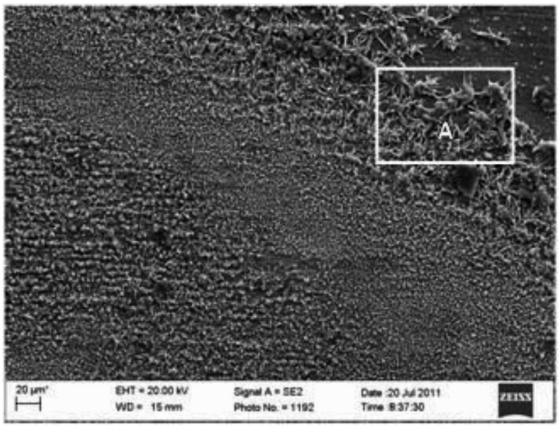

Fig. 12. The surface inside the rectangle #B according to Fig. 10

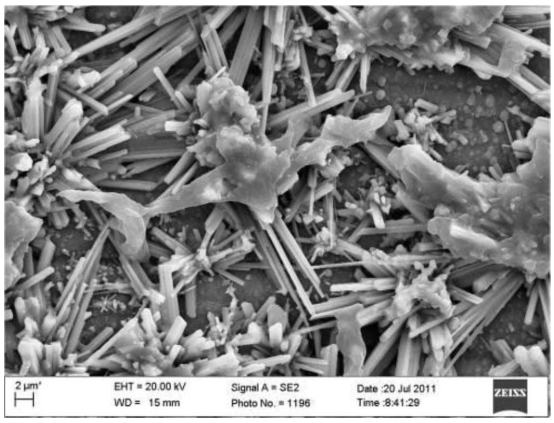

Fig. 13. The surface inside the rectangle #A according to Fig. 12

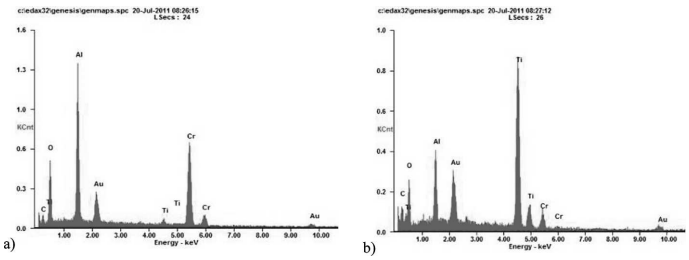

Fig. 14. EDX analysis results: (a) in area inside the rectangle #A according to Fig. 10 and (b) in area inside the rectangle #B according to Fig. 10

The cross-section of the scale formed on Ti-46Al-7Nb-0,7Cr-0,1Si-0,2Ni coated with AlCrN is shown in Fig. 15÷16. Such a structure of the sublayer proves that

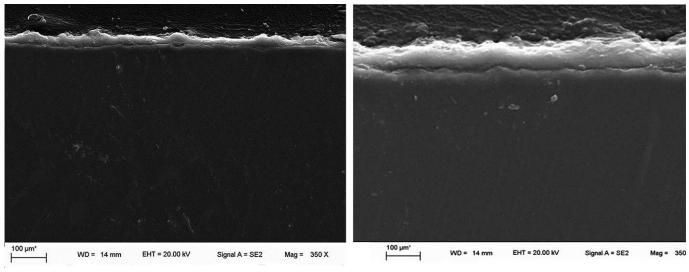

Fig. 15. Cross-section of the scale formed on Ti-46Al-7Nb-0,7Cr-0,1Si-0,2Ni coated with AlCrN after isothermal oxidation in air: (a) at 900°C; (b) at 950

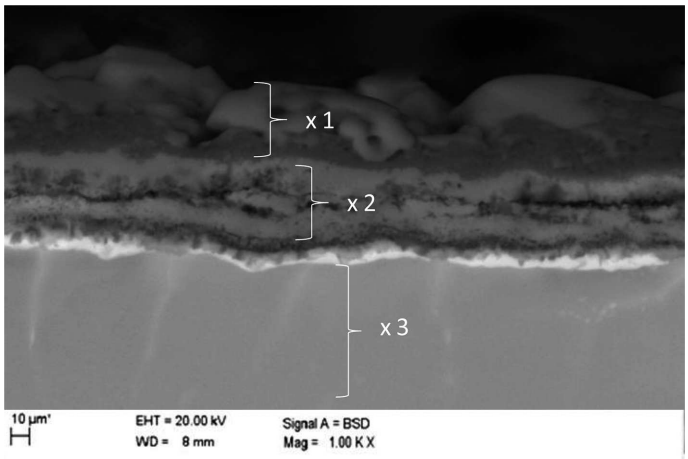

Fig. 16. Cross-section of the scale formed on Ti-46Al-7Nb-0,7Cr-0,1Si-0,2Ni coated with AlCrN after isothermal oxidation in air at 950°C

they have a multi-phase nature. The layered nature and the morphology of the products does not differ regardless of the temperature of the process.

The high temperature of oxygen affecting the AlCrN layer causes the formation of scale, presumably consisting of Cr_2O_3 and Al_2O_3 (that presumption is supported by the performed microanalyses of chemical composition).

In the case of the alloy with a deposited coating the oxidation mechanism occurred as a result of in-core diffusion of oxygen and ex-core diffusion of aluminium and chromium. However, the faster diffusion of chromium [20] led to the formation of Cr_2O_3 dispersed in the outer layer of the scale.

Despite the high resistance to oxidation of the Ti-Al alloy coated with AlCrN, trace elements of rutile can be detected in the scale (Fig. 13). The formation of rutile efflorescences may be explained by the method of fixing the samples during the coating deposition. Efflorescences turn up in the spots where the substrate was insufficiently protected with the coating (in the area where a grip, holding the sample during the coating deposition, was placed.) It only confirms the conclusion that the AlCrN coating has a positive impact on restricting the out-core diffusion of titanium during the oxidation.

To sum up, it may be concluded that the occurring processes lead to the formation of the scale made of a mixture of oxide layer containing aluminium and chromium (from the coating) and titanium which diffused ex-core from the metallic

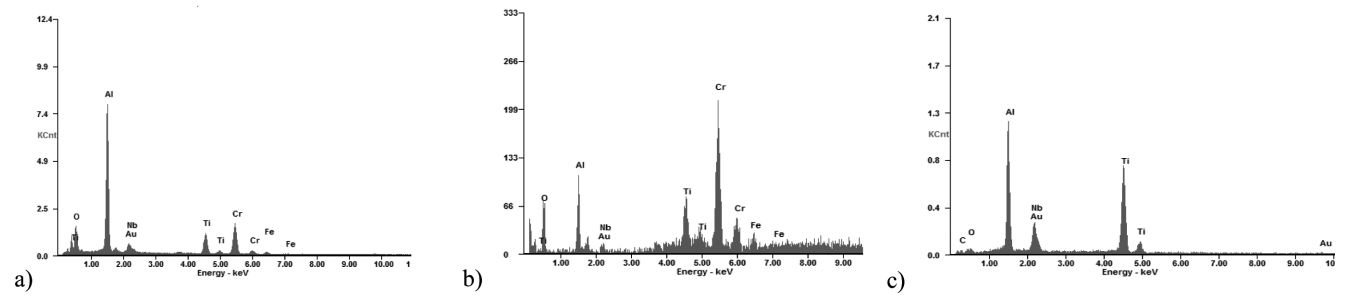

Fig. 17. EDX analysis results: (a) in area #1 according to Fig. 16; (b) in area #2 according to Fig. 16; (c) in area #3 according to Fig. 16

substrate where it was not protected with the coating. Taking into consideration the presented results, it can be concluded that the AlCrN coating caused the improvement of the heat resistance of the base alloy without any interference with its mechanical properties.

The oxidation mechanism was dominated by an inward diffusion of oxygen and outward diffusion of chromium and aluminium [20, 22÷23]. Rapid outward diffusion of chromium can result in the formation of Cr_2O_3 grains dispersed in the outer oxide layer [20]. The mixed chromia/alumina scale was found to be an effective diffusion barrier, retarding or preventing further oxidation of the coating [21÷22].

The aluminia/chromia scale was also an effective barrier to oxygen diffusion, preventing oxidation of the substrate material. As reported in the literature, the exposure of AlCrN thin films to high temperature in air caused formation of mixed Cr_2O_3 and Al_2O_3 scales [20÷21, 23].

Analysing the research results it was concluded that the product growth rate is highly dependent on the temperature. Diffusion processes activate along with the temperature rise and oxidation time, which is shown by higher mass gains (Fig. 5) with greater thickness of the scale (Fig. 15). It was also observed that for the alloy coated with AlCrN, the formed oxide layers are well adhesive to the metallic substrate throughout the entire time of the test in this temperature range. Whereas for the initial state (uncoated) alloy, "deferred" chipping of the scale was determined as soon as within 24 hours from the test completion.

It can be seen that, at a higher temperature, in the area of product-substrate phase boundary micropores develop more actively (Fig. 15b). More active development of micropores is linked to the increase of the oxidation temperature which decidedly accelerates the diffusion processes in the oxidized layer and metallic substrate. Thus, ex-core diffusion of metal ions is accompanied by an increase in the concentration of vacancies at the product-substrate boundary up to the point of cohesion breach. Compressive stresses generated upon the oxidation and the cooling down of the sample to the room temperature cause the buckling of the layer and its removal from the substrate.

The band contrast of the products' layer and metallic substrate calls for examining the chemical composition of individual sublayers. For this purpose microanalyses were carried out in some points of the layer. The chemical composition of the marked spots was shown in Fig. (17a÷c).

Microstructural analyses showed that depending on the process temperature, a scale was formed consisting of a thick outer layer – ranging between about 35 to 50 μm (Fig. 15a÷b). Along with increasing the time of the heat treatment, the growth of the scale thickness was established. This layer was composed of alternating bright and dark grains. Detailed analysis of the chemical composition proved the presence of the scale on the coating made mainly of protective layer of oxides rich in aluminium and chromium and an amount of titanium (Fig. 17a and 17b). In the area of the coating the presence of voids was also established. In the transitional zone between the substrate and the coating, numerous fine-disperse secretions rich in titanium, aluminium, and chromium were revealed. The analysis of the chemical composition in the area of alloy substrate was presented in Fig. 17c.

The presence of carbon (C) and iron (Fe) in the results of X-ray microanalysis is caused by organic pollutions occurring on the surface of the sample and taken into consideration in the quantitative microanalysis. Chemical composition microanalyses of the surface of the oxidized alloy show traces of Au (visible reflections in Fig. 17). The presence of Au reflections on the radiation spectrum is a consequence of the methodology of the preparation of samples for microscopic examination.

4. Summary and conclusions

The heat resistance of the alloy coated with a protective film of AlCrN is higher than in the case of initial state alloy. This coating adds to reducing the oxidation rate and causes the mass gain to be smaller compared with the uncoated layer.

Chromium as the basic ingredient of the deposited coating is an element which reacts with air, undergoes passivation, so chromium oxide (III) is formed which becomes a protective coating. Besides that, it creates Laves' phases – Ti(Cr) with low permeability of oxygen. As a consequence of oxidation, aluminium activity intensified and the resulting increase in the tendency for its selective oxidation takes place. The dominating ingredient of the formed scale is Al and Cr as expected, which has a positive impact of the applied coating on increasing the heat resistance of the alloy. Despite high oxidation resistance of AlCrN coating, trace elements of rutile can be detected in the scale, which is generated due to ex-core diffusion of titanium.

Taking into consideration the presented results, it can be concluded that the coating of AlCrN caused the heat resistance of the substrate alloy to increase without interference with its mechanical properties, which can be a foundation for its prospective application.

Acknowledgements

The research study was financed from the funds for science in 2010-2011 as research project no. IP 2010 023870.

REFERENCES

[1] E.A Loria, Intermetallic **8**, 1339-1345 (2000).
[2] W. Szkliniarz, The alloys from the binary system of Ti-Al, Z. Bojar, W. Przetakiewicz, (Eds.), (in Polish), Technical Military Academy, Warsaw, Chapter 2.2, 66-68 (2006).
[3] A. Hernas, Heat-resistance of steel and alloys (in Polish), Silesian University of Technology, Gliwice (1999).
[4] S. Krol, M. Prażmowski, Material Engineering **3** , 456-459 (2006), (in Polish).
[5] M. Yoshihara, Y.W. Kim, Intermetallic **13**, 952-958 (2005).
[6] Y. Shen, F. Wang, Material Science **39**, 6583-6589 (2004).
[7] M. Schmitz-Niederau, M. Schutze, Oxidation of Metals **52**, 225-240 (1999).
[8] N. Toshio, I. Takeshi, M. Yatagai, T. Yoshioka, Intermetallic **8**, 371-379 (2000).
[9] B.G. Kim, G.M. Kim, C.J. Kim, Scripta Metallurgica et Materiala **33**, 1117-1125 (1995).
[10] S. Król, Protection against Corrosion **11s/A** (in Polish), 194-198 (2005).

[11] Y. Wu, K. Hagihara, Y. Umakoshi, Intermetallic **13**, 879-884 (2005).
[12] S. Król, J. Małecka, L. Zemcik, Protection against Corrosion **11s/A** (in Polish), 124-128 (2007).
[13] J. Małecka, W. Grzesik, A. Hernas, Corrosion Science **52**, 263-272 (2010).
[14] Z. Tang, F. Wang, W. Wu, Material Science Engineering **A276**, 70-75 (2000).
[15] L. Swadźba, G. Moskal, M. Hetmańczyk, B. Mendala, G. Jarczyk, Surface and Coatings Technology **184**, 93-101 (2004).
[16] Z. Liu, G. Wang, Material Science Engineering A **397**, 50-57 (2005).
[17] G.S. Fox-Rabinovich, D.S. Wilkinson, S.C. Veldhuis, G.K. Dosbaeva, G.C. Weatherly, Intermetallic **14**, 189-197 (2006).
[18] T. Izumi, T. Nishimoto, T. Narita, Superior long-term oxidation resistance of Ni-Al coated TiAl alloys, Intermetallic **13**, 727-732 (2005).
[19] J. Małecka, Corrosion Science **63**, 287-292 (2012).
[20] M. Zhu, M. Li, Y. Zhou, Surface and Coatings Technology **201**, 2878-2886 (2006).
[21] O. Banakh, P.E. Schmid, R. Sanjies, F. Levy, Surface and Coatings Technology **163-164**, 57-61 (2003).
[22] J.L. Endrino, G.S. Fox-Rabinovich, A. Reiter, S.V. Veldhuis, R. Escobar Galindo, J.M. Albella, et al., Surface & Coatings Technology **201**, 4505-4511 (2007).
[23] E. Huber, S. Hofmann, Surface and Coating Technology **68-69**, 64-69 (1994).

Received: 10 September 2013.